

# Thermal diffusivity of samarium–gadolinium zirconate solid solutions

W. Pan\*, C.L. Wan, Q. Xu, J.D. Wang, Z.X. Qu

State Key Laboratory of New Ceramics and Fine Processing, Department of Materials Science and Engineering,  
Tsinghua University, Beijing 100084, China

Available online 9 December 2006

## Abstract

We synthesized samarium–gadolinium zirconate solid solutions and determined their thermal diffusivities, Young's moduli and thermal expansion coefficients, which are very important for their application in thermal barrier coatings. Samarium–gadolinium zirconate solid solutions have extremely low thermal diffusivity between 20 and 600 °C. The solid solutions have lower Young's moduli and higher thermal expansion coefficients than those of pure samarium and gadolinium zirconates. This combination of characteristics is promising for the application of samarium and gadolinium zirconates in gas turbines. The mechanism of phonon scattering by point defects is discussed.

© 2006 Elsevier B.V. All rights reserved.

*Keywords:* Thermal diffusivity; Thermal barrier coatings; Samarium–gadolinium zirconate

## 1. Introduction

In order to improve the thermal efficiency and reliability of gas turbines, thermal barrier coatings (TBCs) have been developed to protect the hot-section of the metallic components and permit increase in the engine inlet gas temperature [1–5]. Commercially, the most commonly used TBC has been yttria stabilized zirconia (8-YSZ) [1–4]. Several processes [6,7] have been developed to coat YSZ on the metallic bond-coat; these include electron-beam physical vapor deposition (EB-PVD), plasma enhanced chemical vapor deposition (PE-CVD), air plasma spraying (APS). However, YSZ still has some disadvantage when exposed to high temperature (>1200 °C) for extended intervals, because phase transition and shrinkage can damage the coatings [1,8]. Hence, in recent years there has been considerable interest in developing new TBCs with lower thermal conductivity and higher stability at elevated temperature, with the goal of achieving further improvements in engine performance.

Among the thousands of possible candidates, initial research has focused on fluorite- and pyrochlore-structured oxide materials related to zirconia, doped with rare earth elements [2,8–15]. Compounds with the formula  $M_2Zr_2O_7$  ( $M = La, Nd, Gd, Sm, \dots$ ) have remarkably lower thermal conductivity than YSZ, due to their complex structure, large atomic mass and high concen-

tration of oxygen vacancy. Furthermore, they are chemically stable at high temperatures [8–11,13,14]. Thermal conductivities for zirconates doped with Gd, Eu, Sm, Nd, Er, Dy, Yb and La range from 1.1 to 1.8 W/mK at temperatures between 700 and 1200 °C [8–11,13,14].

This paper reports synthesis of samarium and gadolinium zirconates and their solid solution materials, the thermal conductivities and related physical properties of these materials, and clarifies the effects of doping element on the phonon scattering and thermal conduction behavior. The selected end lanthanide zirconates for the solid solution were  $Gd_2Zr_2O_7$  and  $Sm_2Zr_2O_7$ .

## 2. Experimental procedure

The  $(Sm_{1-x}Gd_x)_2Zr_2O_7$  ( $x = 0, 0.2, 0.4, 0.6, 0.8, 1$ ) specimens were synthesized by a solid reaction method. For each composition,  $Gd_2O_3$  and  $Sm_2O_3$  were weighed and mixed with  $ZrO_2$  (purity of all chemicals 99.99%, Rare Earth Chem. Co., China) by ball milling. The mixed powders were dry-pressed into disk shapes and sintered at 1600 °C for 20 h. The phases of the sintered bulk materials were then characterized by X-ray diffraction (XRD, D/max-RB, Japan), and the microstructure of the specimen was observed by scanning electron microscopy (SEM, JEOL-6301F, Japan). The density  $\rho$  (g/cm<sup>3</sup>) of the sintered bulk specimen was measured according to Archimedes' principle. The theoretical densities of each solid solution composition were calculated using lattice parameters acquired from XRD results and the molecular weight of the unit cell. Ther-

\* Corresponding author. Tel.: +86 10 62772858; fax: +86 10 62771160.  
E-mail address: [panw@mail.tsinghua.edu.cn](mailto:panw@mail.tsinghua.edu.cn) (W. Pan).

mal expansion coefficients were measured using a dilatometer (NETZSCH DIL 402EP, Germany). Thermal diffusivity ( $\kappa$ ) was measured using the laser-flash method (NETZSCH LFA 427, Germany). Specific heat capacity ( $C_p$ ) of the specimen was measured by DSC instrument (NETZSCH DSC204, Germany). Thermal conductivity ( $k'$ ) of the sintered specimen was then determined using formula (1):

$$k' = \kappa \times C_p \times \rho \quad (1)$$

Since the sintered specimen still contains micro-pores, thermal conductivity of the fully dense solid ( $k$ ) was further normalized by the formula [16]:

$$\frac{k'}{k} = 1 - \frac{4}{3}\phi \quad (2)$$

where  $\phi$  is the porosity of the sintered specimen. The elastic constants and Poisson ratio were acquired from the longitudinal and transverse acoustic velocities, which were measured ultrasonically (Ultrasonic Pulser/Receiver Model 5900 PR, Panametrics) and these values of elastic constants were extrapolated to fully density by the formula [17]:

$$E_0 = \frac{E(\phi)}{(1 - \phi^{2/3})^{1.21}} \quad (3)$$

### 3. Results and discussion

#### 3.1. Structural analysis

The ion radius difference of  $\text{Sm}^{3+}$  and  $\text{Gd}^{3+}$  is 2%, and they have the same valency in the  $\text{Sm}_2\text{Zr}_2\text{O}_7$  and  $\text{Gd}_2\text{Zr}_2\text{O}_7$  compounds, but  $\text{Sm}_2\text{Zr}_2\text{O}_7$  is a pyrochlore and  $\text{Gd}_2\text{Zr}_2\text{O}_7$  is a fluorite; these structures can be distinguished by the (3 3 1) peak from the XRD patterns of synthesized  $(\text{Sm}_{1-x}\text{Gd}_x)_2\text{Zr}_2\text{O}_7$  specimens (Fig. 1). Except for  $\text{Gd}_2\text{Zr}_2\text{O}_7$  all  $(\text{Sm}_{1-x}\text{Gd}_x)_2\text{Zr}_2\text{O}_7$  specimens ( $x=0, 0.2, 0.4, 0.6, 0.8$ ) are in the pyrochlore structure.  $\text{Gd}_2\text{Zr}_2\text{O}_7$  has a defective fluorite-type structure, and incorporation of  $\text{Sm}^{3+}$ , transforms it into an ordered pyrochlore-type structure. The (3 3 1) peak characterizes the superstructure

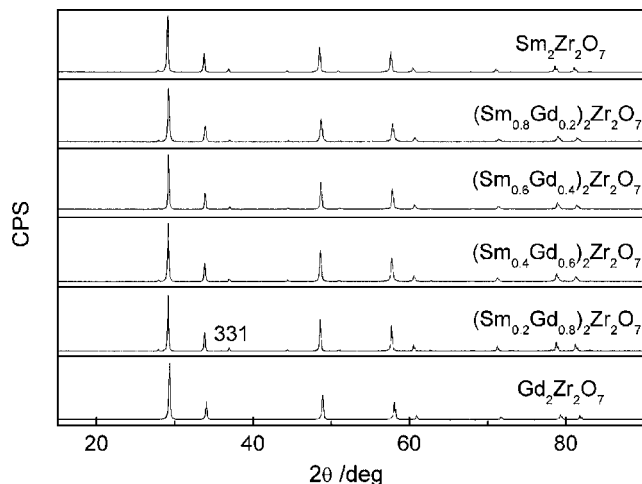


Fig. 1. XRD patterns of  $(\text{Sm}_{1-x}\text{Gd}_x)_2\text{Zr}_2\text{O}_7$  ( $x=0, 0.2, 0.4, 0.6, 0.8, 1$ ).

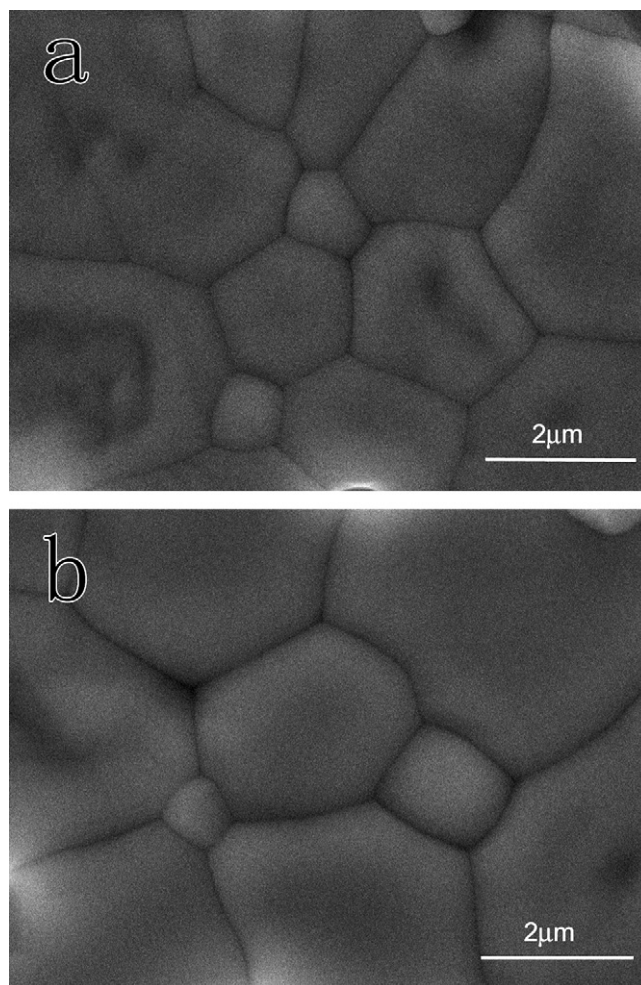


Fig. 2. Typical SEM features of the sintered  $(\text{Sm}_{1-x}\text{Gd}_x)_2\text{Zr}_2\text{O}_7$  TBC materials: (a)  $(\text{Sm}_{0.8}\text{Gd}_{0.2})_2\text{Zr}_2\text{O}_7$  and (b)  $(\text{Sm}_{0.2}\text{Gd}_{0.8})_2\text{Zr}_2\text{O}_7$ .

of the ordered pyrochlore-type structure and can be used to distinguish between pyrochlore and fluorite structure [18].

The SEM features of the sintered compounds are shown in Fig. 2. Almost fully densified  $(\text{Sm}_{1-x}\text{Gd}_x)_2\text{Zr}_2\text{O}_7$  were obtained, and the average grain size is about 5–10  $\mu\text{m}$ . The relative densities of the sintered specimens were higher than 98%.

#### 3.2. Thermal conductivity

Normalized thermal conductivities ( $k$ ) of  $\text{Sm}_2\text{Zr}_2\text{O}_7$  and  $\text{Gd}_2\text{Zr}_2\text{O}_7$  between 20 and 1400  $^\circ\text{C}$  both decreased with increasing temperature (Fig. 3), and the lowest value is close to 1.2 W/mK. The small increase of the value at higher temperatures might be due to thermal radiation produced by photons.

The thermal diffusivities of the solid solutions  $(\text{Sm}_{1-x}\text{Gd}_x)_2\text{Zr}_2\text{O}_7$  are lower than those of  $\text{Sm}_2\text{Zr}_2\text{O}_7$  and  $\text{Gd}_2\text{Zr}_2\text{O}_7$  between 20 and 600  $^\circ\text{C}$  (Fig. 4). The minimum observed thermal diffusivity of  $(\text{Sm}_{1-x}\text{Gd}_x)_2\text{Zr}_2\text{O}_7$  occurred at  $x=0.4$ . The reduced thermal diffusivity of the solid solutions may correlate with their lattice imperfections. Resistance to phonon transfer in electrically insulating solids is related to intrinsic phonon scattering,

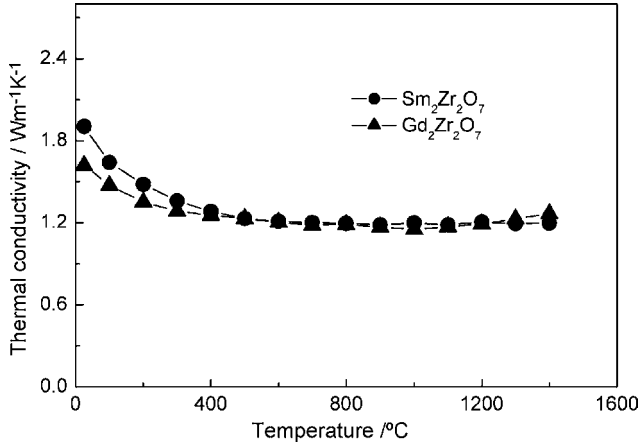


Fig. 3. Thermal conductivities of  $\text{Sm}_2\text{Zr}_2\text{O}_7$  and  $\text{Gd}_2\text{Zr}_2\text{O}_7$ .

point defect scattering and grain boundary scattering, which result in thermal diffusivity reduction [19]. As seen from Fig. 2, grain size in the present study is much larger than the phonon mean free path (i.e., <1 nm), hence the resistance for the phonon transfer in the solid solution comes mainly from intrinsic phonon scattering and point defect scattering. The lattice imperfections in the solid solution are caused by substitution of  $\text{Sm}^{3+}$  by  $\text{Gd}^{3+}$  in  $\text{Sm}_2\text{Zr}_2\text{O}_7$  or substitution of  $\text{Gd}^{3+}$  by  $\text{Sm}^{3+}$  in  $\text{Gd}_2\text{Zr}_2\text{O}_7$ . Thermal conduction owing to the changes of lattice vibrations may be affected by point defect scattering for phonons including mass differences (mass fluctuation) [20,21], and size and interatomic coupling force differences (strain field fluctuations) [22], respectively, which alter the mean free path of the phonon ( $\lambda$ ), and the velocity of the phonon ( $v$ ).

For a compound  $\text{U}_x\text{V}_y$ , which has a crystal structure comprised of U and V sites, the imperfection parameter  $\Gamma$  is expressed by [23]:

$$\Gamma_{\text{U}_x\text{V}_y} = \frac{x}{x+y} \left( \frac{M_{\text{U}}}{\bar{M}} \right)^2 \Gamma_{\text{U}} + \frac{y}{x+y} \left( \frac{M_{\text{V}}}{\bar{M}} \right)^2 \Gamma_{\text{V}} \quad (4)$$

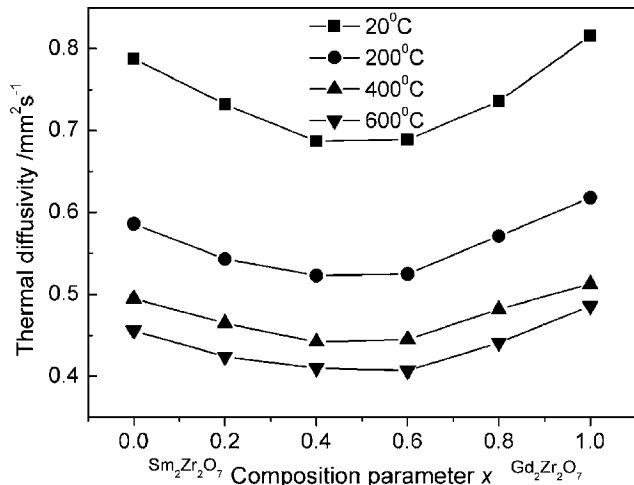


Fig. 4. Thermal diffusivities of  $(\text{Sm}_{1-x}\text{Gd}_x)_2\text{Zr}_2\text{O}_7$  specimens measured at different temperatures.

where  $M_{\text{U}}$  and  $M_{\text{V}}$  are the average mass of U and V sites, respectively, and  $\bar{M} = (xM_{\text{U}} + yM_{\text{V}})/(x+y)$ .  $\Gamma_{\text{U}}$  and  $\Gamma_{\text{V}}$  represent the individual imperfection parameters of those two sites. For the pyrochlore-type solid solution  $(\text{Sm}_{1-x}\text{Gd}_x)_2\text{Zr}_2\text{O}_7$ , Sm and Gd are substituted for each other and there are four crystallographic sites, including the sites of (Sm,Gd), Zr, O and oxygen vacancy  $\text{V}_{\text{O}}$ , with their respective degeneracy of 2, 2, 7 and 1, respectively. Then,

$$\Gamma_{(\text{Sm}_x\text{Gd}_{1-x})_2\text{Zr}_2\text{O}_7} = \frac{2}{12} \left( \frac{M_{\text{Sm,Gd}}}{\bar{M}} \right)^2 \Gamma_{(\text{Sm,Gd})} + \frac{2}{12} \left( \frac{M_{\text{Zr}}}{\bar{M}} \right)^2 \Gamma_{\text{Zr}} + \frac{7}{12} \left( \frac{M_{\text{O}}}{\bar{M}} \right)^2 \Gamma_{\text{O}} + \frac{1}{12} \left( \frac{M_{\text{V}_{\text{O}}}}{\bar{M}} \right)^2 \Gamma_{\text{V}_{\text{O}}} \quad (5)$$

where  $\bar{M}$  is the average mass of  $(\text{Sm}_{1-x}\text{Gd}_x)_2\text{Zr}_2\text{O}_7$ ,  $M_{\text{Sm,Gd}}$ ,  $M_{\text{Zr}}$ ,  $M_{\text{O}}$  and  $M_{\text{V}_{\text{O}}}$  are the mass of (Sm,Gd), Zr, O and oxygen vacancy  $\text{V}_{\text{O}}$  site. Here  $M_{\text{V}_{\text{O}}}$  is considered to be zero. Since there is no change at the sites of Zr, O and oxygen vacancy when the substitution between Sm and Gd occurs,  $\Gamma_{\text{Zr}} = \Gamma_{\text{O}} = \Gamma_{\text{V}_{\text{O}}} = 0$ , gives:

$$\Gamma_{(\text{Sm}_x\text{Gd}_{1-x})_2\text{Zr}_2\text{O}_7} = \frac{1}{6} \left( \frac{M_{\text{Sm,Gd}}}{\bar{M}} \right)^2 \Gamma_{(\text{Sm,Gd})} \quad (6)$$

$$\Gamma_i = f_i \left\{ \left( \frac{\Delta M_i}{M} \right)^2 + 2 \left[ \left( \frac{\Delta G_i}{G} \right) - 6.4\gamma \left( \frac{\Delta \delta_i}{\delta} \right) \right]^2 \right\} \quad (7)$$

$$\Gamma_{(\text{Sm,Gd})} = \sum_i \Gamma_i \quad (8)$$

where the subscript  $i$  denotes Sm or Gd,  $\Gamma_i$  characterizes the scattering cross-section of the impurity atom  $i$ ,  $f_i$  the fractional concentration of the substitution atom,  $M$  and  $\delta$  the average mass and radius of the substituted site in the host lattice,  $\delta_i$  the radius of the substitute in the host lattice,  $G_i$  an average stiffness constant of the nearest neighbor bonds from the substitute to the host lattice,  $G$  the corresponding quantity of the host atoms,  $\Delta G = G_i - G$ ,  $\Delta M = M_i - M$ ,  $\Delta \delta_i = \delta_i - \delta$  and  $\gamma$  is the average anharmonicity of the bonds (the Grüneisen parameter). Obviously,  $\Gamma_i$  is a function of the concentration of the substitute atom.

Above the Debye temperature, the ratio of the lattice thermal diffusivity of a material containing defects with that of the parent material can be written as [24]:

$$\frac{\kappa}{\kappa_{\text{P}}} = \frac{\tan^{-1}(u)}{u} \quad (9)$$

Here  $\kappa$  and  $\kappa_{\text{P}}$  are the lattice thermal diffusivities of the defected and parent materials, respectively, and the parameter  $u$  is defined by [24]

$$u = \left( \frac{\pi^2 \theta_{\text{D}} \Omega}{h v^2} \kappa_{\text{P}} \Gamma \right)^{1/2} \quad (10)$$

The symbols  $h$ ,  $v$ ,  $\Omega$ ,  $\theta_{\text{D}}$  stand for the Plank constant, lattice sound velocity, average volume per atom and the Debye tem-

perature which could be estimated by [25]

$$\theta_D = \frac{h\nu}{k_B} \left( \frac{6\pi^2}{\Omega} \right)^{1/3} \quad (11)$$

where  $k_B$  denotes the Boltzmann's constant. In the present study, when Sm is partially substituted by Gd in  $\text{Sm}_2\text{Zr}_2\text{O}_7$ , the point defects produced and the imperfection parameter  $I$  are both functions of the substitution concentration. Thermal diffusivity was highest in pure compounds, and decreased as impurities (either Sm or Gd) were introduced into the crystals.

### 3.3. Young's modulus

At room temperature, the Young's moduli of all the solid solutions are lower than those of pure  $\text{Sm}_2\text{Zr}_2\text{O}_7$  and  $\text{Gd}_2\text{Zr}_2\text{O}_7$  (Fig. 5). The strain field fluctuations induced by solute atoms may modify the elastic properties of solid solutions, and in turn affect their thermal transport properties. Solute atoms entering interstitial sites always cause hardening of the crystal. Ibegazene et al. [26] substituted zirconia in YSZ with hafnia and observed progressive increase of Young's modulus in the solid solutions, due to formation of new phases. In the present study,  $\text{Sm}^{3+}$  substituted by  $\text{Gd}^{3+}$  or vice versa did not create new phases compared with the end compounds. A reduced Young's modulus was observed. We infer that the size and coupling force misfit induced by substitution atoms have "softened" the lattice and that the strain field fluctuation acts in the form of lattice relaxation. The relaxation reduces the propagation velocity of phonons and in turn suppresses the thermal conduction in the investigated solid solutions. Clarke [27] deduced an expression for the lattice thermal conductivity as:

$$k \propto \frac{\rho^{1/6} E^{1/2}}{(M/m)^{2/3}} \quad (12)$$

where  $\rho$  is the density,  $E$  represents the Young's modulus,  $M$  the atomic weight of the molecule of the compound and  $m$  is the number of atoms in the molecule. Eq. (11) indicates that a

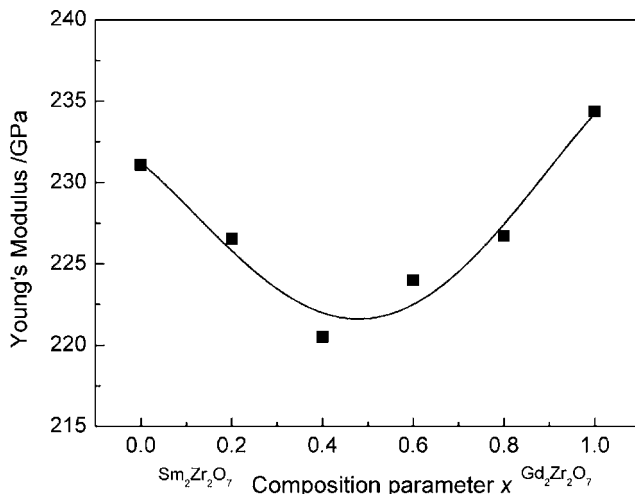


Fig. 5. Young's modulus of  $(\text{Sm}_{1-x}\text{Gd}_x)_2\text{Zr}_2\text{O}_7$  specimens measured at room temperature.

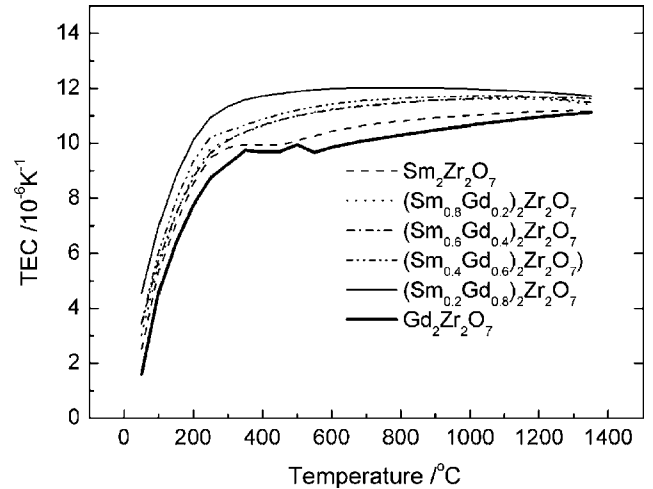


Fig. 6. Thermal expansion coefficients of  $(\text{Sm}_{1-x}\text{Gd}_x)_2\text{Zr}_2\text{O}_7$  at different temperatures.

smaller value of  $E$  yields a lower thermal diffusivity, and it is consistent with the results shown in Fig. 4, which was measured using the laser-flash method. Besides, a small Young's modulus is favored in TBC applications, as it produces smaller residual stresses in the coating system under the service conditions and results in better thermal–mechanical stability than compounds with higher Young's moduli [10,26,28].

### 3.4. Thermal expansion coefficient

The thermal expansion coefficient is also a very important physical property for TBC materials. Because the thermal expansion coefficient of ceramic materials is usually much smaller than that of metallic materials, the residual stresses between the TBC material and the metallic bond-coat increases and induces cracks at the interface of the TBC and bond-coat. The thermal expansion coefficient of the  $(\text{Sm}_x\text{Gd}_{1-x})_2\text{Zr}_2\text{O}_7$  solid solutions (Fig. 6) is on the same order of conventional TBC (YSZ,  $\sim 10 \times 10^{-6} \text{ K}^{-1}$ ) [1] and  $(\text{Sm}_{0.2}\text{Gd}_{0.8})_2\text{Zr}_2\text{O}_7$  shows the highest value in the solid solutions. Compared with end compositions of  $\text{Sm}_2\text{Zr}_2\text{O}_7$  and  $\text{Gd}_2\text{Zr}_2\text{O}_7$ , thermal expansion coefficients of the solid solutions are all apparently improved, which possibly originated from the enhanced anharmonicity aroused by point defects.

## 4. Conclusion

Samarium and gadolinium zirconates and their solid solution materials have been successfully synthesized. Samarium zirconates and the solid solutions  $(\text{Sm}_x\text{Gd}_{1-x})_2\text{Zr}_2\text{O}_7$  have a pyrochlore type structure except for  $\text{Gd}_2\text{Zr}_2\text{O}_7$ . The solid solutions had extremely low thermal diffusivity in the temperature range 20–600 °C, compared with the end compounds  $\text{Sm}_2\text{Zr}_2\text{O}_7$  and  $\text{Gd}_2\text{Zr}_2\text{O}_7$ . Point defect phonon scattering was identified as the main reason for the low thermal diffusivity of the solid solutions. Minimum values of Young's modulus in the solid solutions were also observed; these may be correlated with the strain field fluctuation and to the minimum thermal diffusivity. The solid

solutions even have higher thermal expansion coefficients than those of the end compounds, due to the enhanced anharmonicity by point defects.  $(\text{Sm}_{1-x}\text{Gd}_x)_2\text{Zr}_2\text{O}_7$  ( $x = 0.2, 0.4, 0.6, 0.8$ ) shows promise as a TBC material.

### Acknowledgements

This work is supported by National Natural Science Foundation of China (Nos. 50232020 and 50572042).

### References

- [1] D.R. Clarke, S.R. Phillpot, *Mater. Today* 8 (2005) 22.
- [2] X.Q. Cao, R. Vassen, D. Stoeber, *J. Eur. Ceram. Soc.* 24 (2004) 1–10.
- [3] U. Schulz, C. Leyens, K. Fritscher, M. Peters, B. Saruhan-Brings, O. Lavigne, J.M. Dorvaux, M. Poulain, R. Mevrel, M.L. Caliez, *Aerosp. Sci. Technol.* 7 (2003) 73–80.
- [4] N.P. Padture, M. Gell, E.H. Jordan, *Science* 296 (2002) 280–284.
- [5] F. Cernuschi, P. Bianchi, M. Leoni, P. Scardi, *J. Therm. Spray Technol.* 8 (1999) 102–109.
- [6] R.A. Miller, *Surf. Coat. Technol.* 30 (1987) 1–11.
- [7] W.A. Nelson, R.M. Orenstein, *J. Therm. Spray Technol.* 6 (1997) 176–180.
- [8] R. Vassen, X.Q. Cao, F. Tietz, D. Basu, D. Stover, *J. Am. Ceram. Soc.* 83 (2000) 2023–2028.
- [9] Q. Xu, W. Pan, J.D. Wang, C.L. Wan, L.H. Qi, H.Z. Miao, K. Mori, T. Torigoe, *J. Am. Ceram. Soc.* 89 (2006) 340–342.
- [10] J. Wu, X.Z. Wei, N.P. Padture, P.G. Klemens, M. Gell, E. Garcia, P. Miranzo, M.I. Osendi, *J. Am. Ceram. Soc.* 85 (2002) 3031–3035.
- [11] J. Wu, N.P. Padture, P.G. Klemens, M. Gell, E. Garcia, P. Miranzo, M.I. Osendi, *J. Mater. Res.* 17 (2002) 3193–3200.
- [12] S. Raghavan, H. Wang, W.D. Porter, R.B. Dinwiddie, M.J. Mayo, *Acta Mater.* 49 (2001) 169–179.
- [13] G. Suresh, G. Seenivasan, M.V. Krishnaiah, P.S. Murti, *J. Alloys Compd.* 269 (1998) L9–L12.
- [14] G. Suresh, G. Seenivasan, M.V. Krishnaiah, P.S. Murti, *J. Nucl. Mater.* 249 (1997) 259–261.
- [15] M.N. Rahaman, J.R. Gross, R.E. Dutton, H. Wang, *Acta Mater.* 54 (2006) 1615–1621.
- [16] K.W. Schlichting, N.P. Padture, P.G. Klemens, *J. Mater. Sci.* 36 (2001) 3003–3010.
- [17] M. Asmani, C. Kermel, A. Leriche, M. Ourak, *J. Eur. Ceram. Soc.* 21 (2001) 1081–1086.
- [18] B.J. Wuensch, K.W. Eberman, C. Heremans, E.M. Ku, P. Onnerud, E.M.E. Yeo, S.M. Haile, J.K. Stalick, J.D. Jorgensen, *Solid State Ionics* 129 (2000) 111–133.
- [19] R. Berman, *Thermal Conduction in Solids*, Clarendon Press, Oxford, 1976, pp. 45–101.
- [20] B. Abeles, *Phys. Rev.* 131 (1963) 1906–1911.
- [21] G. Slack, *Phys. Rev.* 105 (1957) 829–834.
- [22] J. Yang, G.P. Meisner, L. Chen, *Appl. Phys. Lett.* 85 (2004) 1140–1142.
- [23] G. Slack, *Phys. Rev.* 126 (1962) 427–432.
- [24] J. Callaway, H.C. von Baeyer, *Phys. Rev.* 120 (1960) 1149–1154.
- [25] C. Kittel, *Introduction to Solid State Physics*, Wiley, New York, 1996, pp. 122.
- [26] H. Ibegazene, S. Alperine, C. Diot, *J. Mater. Sci.* 30 (1995) 938–951.
- [27] D.R. Clarke, *Surf. Coat. Technol.* 163 (2003) 67–74.
- [28] J.A. Thompson, T.W. Clyne, *Acta Mater.* 49 (2001) 1565–1575.